

Coherent Laser Beam Addition: An Application of Binary-Optics Technology

Coherent laser beam addition offers the potential for extremely bright optical sources by combining the power from many individual lasers. Binary-optical elements — surface-relief structures etched into optical substrates by integrated-circuit techniques — have been successfully employed in three optical beam addition systems. The techniques can produce diffraction-limited laser sources from large-scale two-dimensional laser arrays. Future electrooptic systems, ranging from communications to space surveillance, can benefit from the new high-power laser sources made possible by coherent laser beam addition.

Laser light— narrow band, coherent in time and space — forms the basis of many practical sensor and communications systems. Some potential applications, however, demand laser power well above single-laser capabilities. Since all lasers are limited in power by physical constraints (gain saturation, optical damage, heat dissipation, modal purity, etc.), these applications require special addition techniques for harnessing the combined power capability of many lasers.

The optics required for laser addition is often extremely difficult or impossible to fabricate by conventional means. We have developed an alternative technology, called binary optics, to fabricate these complex optical elements. Binary-optical elements (see the box, "What Is Binary Optics?") consist of computer-designed surface-relief structures that use diffraction to modify the phase, amplitude, and polarization of light. We use binary-optics technology to fabricate unique gratings, phase correctors, and microlenses for laser addition applications.

Although laser beam addition can be applied to a wide variety of laser types, it is particularly important for semiconductor diode lasers. Power radiation densities of today's diode lasers are greater than those at the surface of the sun. Yet the very small radiation surface area of a diode laser (typically a few square microns) can reliably produce only about 25 mW of power per diode. The two principal barriers to greater

optical power are catastrophic facet damage caused by thermal runaway at the output facet, and overall device heating.

Arrays of diode lasers can overcome the thermal barriers and produce high output powers. Catastrophic facet damage is avoided by limiting the power of each laser facet, and the problems associated with device heating are alleviated by providing adequate space between lasers, enabling heat sinks to operate efficiently. Quasi-CW powers of over 100 W are currently available from commercial vendors, and larger two-dimensional CW and pulsed arrays are being developed at Lincoln Laboratory as well as other laboratories.

Coherent Combining of Lasers

For some applications, the *power* of the laser source is of primary importance. These applications include illuminators, multimode fiber sources, and laser pumps. High-power AlGaAs laser diode arrays, for example, have been employed as efficient pumps for Nd:YAG (neodymium-doped yttrium aluminum garnet) slab and rod lasers [1]. However, other applications require power concentration in the far field. Such applications include laser radar, optical communications, single-mode fiber sources, and optical printing. Here the most important measure of laser strength is *radiance* (sometimes called brightness). The

What Is Binary Optics?

Binary optics is a diffractive-optics technology that uses computer-designed surface-relief structures and integrated-circuit etching methods to fabricate optical components. While conventional optics uses mechanical polishing to produce a curved surface of the desired profile, binary optics utilizes high-resolution lithography and ion beam etching to transfer a binary surface-relief pattern to a dielectric or metallic substrate. These versatile devices can perform novel optical functions, as well as provide additional design freedom and materials choices for optical design.

A single etching step produces a two-level surface relief, giving rise to the name "binary optics." Many highly efficient (>90%) blaze-like optical elements such as lenses, prisms, beam splitters, beam multiplexers, and filters can be made with binary surfaces for monochromatic applications (see Fig. A). To be efficient, the relief structure must be smaller than or comparable in size to a wavelength of light and it must typically have a half-wave phase depth.

High diffraction efficiency can also be achieved with multilevel relief structures. By repeating the binary etching process at different depths, such multilevel lenses approximate continuous phase surfaces in a stepwise manner (Fig. B). In general, N masks result in $M = 2^N$ phase levels, with a diffraction efficiency η of

$$\eta = \left| \frac{\sin(\pi/M)}{(\pi/M)} \right|^2. \quad (3)$$

Since every etch doubles the number of phase levels, a small

number of etches can produce a highly efficient element; for example, four etching steps result in a 16-level element with an efficiency of 99%.

These multilevel lenses can be made on flat substrates for monochromatic applications. Aspheric optics such as aberration-free laser collimators and anamorphic lenses can be produced on a single plane. For wideband optical systems, hybrid lenses combining refractive and diffractive optics promise significant simplification of conventional imaging. Refraction from a curved substrate provides the majority of the focal power of the lens, and the binary-optics surface-relief pattern provides spherical and chromatic aberration correction. Spherical corrections consist of precisely placed circular phase zones that change radii as a function of position on the lens surface. Such patterns convert a simple spherical lens into an effective asphere. Similarly, an a-chromatic balance can be struck between the dispersion of the refractive lens material and the dispersion of the diffractive pattern etched into the surface by varying the geometric dimensions of the zones, *ie*, ring width, depth, and spacing, irrespective of the intrinsic properties of the substrate material. Thus the dispersion characteristics of the diffractive pattern can be selected to achromatize optical materials.

These corrections have introduced new aspheric design flexibility, new temperature compensation techniques, and materials choices in electrooptic system designs. Infrared materials such as ZnSe and Si

that were previously restricted because of undesirable dispersion characteristics can be achromatized over moderate bandwidths, whereas, in deep-UV applications, usable optical imaging bandwidths can be enhanced a thousandfold.

The uses of binary-optics technology extend beyond lenses and beam addition components. For instance, corrugated surfaces can be produced on a sub-wavelength scale that function as broadband, wide field-of-view, antireflective coatings. The concepts of this approach are vividly demonstrated by the antireflective properties of moths' eyes that, due to their tiny corrugated surfaces, have virtually no reflection in visible light. Other applications that stretch the capabilities of refractive optics are bifocal contact lenses, deep-UV optics for high-resolution lithography, and large arrays of diffraction-limited microlenses each the size of a human hair.

In the early 1970s many of the concepts of binary optics were developed in the form of kinoforms and optically recorded or computer-generated holograms. Since then — by applying VLSI circuit fabrication techniques — the achievements of high fabrication quality ($\lambda/50$) and high diffraction efficiency (99%) have made many applications of diffractive optics feasible in systems. The ability to mass produce diffractive relief elements through replication, embossing, forging, or molding from a single master element gives this technology a significant and still largely untapped potential.

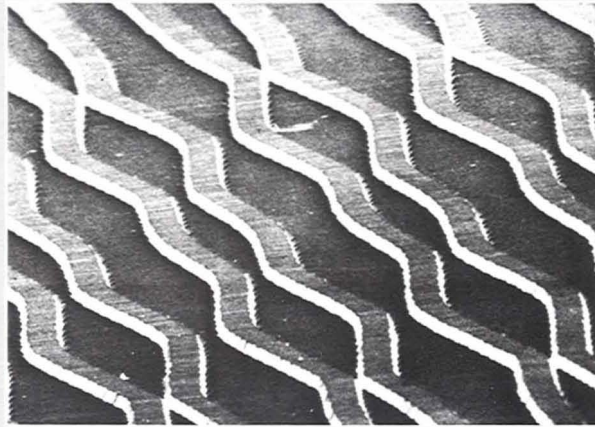


Fig. A — This beam multiplexer is an example of one of the many structures made possible by binary optics. The features are $10\ \mu\text{m}$ wide and $2.5\ \mu\text{m}$ deep. The element is designed for a CO_2 laser with a wavelength of $10.6\ \mu\text{m}$.

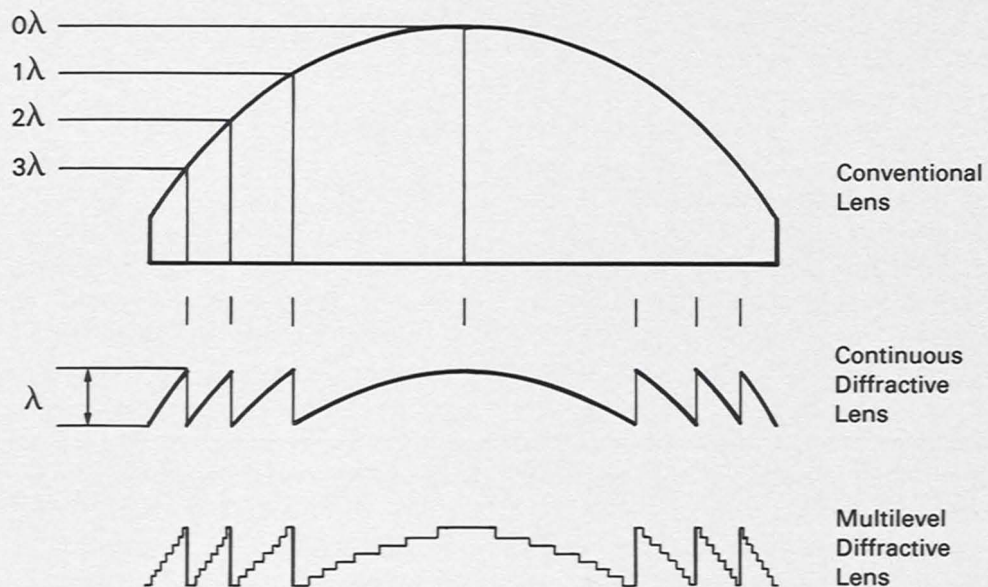


Fig. B — The surface-relief pattern of a diffractive lens is compared to the spherical curvature of a conventional lens. A multilevel diffractive lens approximates this desired surface in a stepwise manner.

radiance of a source is a measure of the power per unit area per unit solid angle.

As an example, a laboratory HeNe laser produces only a few milliwatts of power compared with several watts of optical power from a conventional incandescent light bulb. The laser's radiance, however, is orders of magnitude greater due to the very small beam spread. The high radiance is a consequence of the spatial coherence across the laser beam (phases of two spatially distinct points on the wavefront are locked together), as well as the phase uniformity across the wavefront.

In contrast, an array of mutually incoherent lasers behaves more like the incandescent light bulb, emitting with random phase and frequency variations across the array (although not to the extent of the light bulb). Consequently, although it may provide high optical power, an incoherent array's radiance level is relatively low. Therefore, mutually incoherent laser arrays are not appropriate for applications that require concentrated optical power.

To obtain high radiance from a laser array, three conditions must be met. First, the lasers must be mutually coherent; that is, they must be phase- and frequency-locked to one another. Without coherence, any beam emanating from the array would spread, reducing the radiance of the output. Second, the phase relationship of the lasers must be adjusted to provide the maximum amount of power along the optical axis. It is not sufficient simply to lock the lasers into a steady-state phase relationship. Much as in a phased-array antenna, the laser phases must be adjusted to direct power along the optical axis and, as with a phased array, maximum on-axis power is obtained when the antennas are in phase. Improper phasing leads to beam broadening and reduced on-axis power. Finally, the wavefront emanating from the array must be modified to produce quasi-uniform exit aperture illumination. The light emanating from a laser array contains gaps that result in several diffraction orders called grating lobes, similar to the light distribution from an amplitude diffraction grating. If the wavefront is modified to produce a quasi-uniform output, the off-axis

grating lobes are suppressed, concentrating the optical power in the on-axis lobe.

We have experimented with two fundamentally different methods of beam combining. The first method employs an optical element to superimpose N lasing apertures, converting the laser array into a single emitter with N times the power density. We call this technique *laser beam superposition*. The power per unit area increases by a factor of N while the divergence remains unchanged, resulting in an N -fold increase in radiance.

The second method enlarges the effective size of each lasing aperture until it equals the inter-laser spacing. We call this technique *aperture filling* to describe the quasi-uniform light distribution it produces across the array. As with a diffraction grating of 100% duty factor, the off-axis grating lobes disappear, and the optical power is concentrated in the on-axis beam. Furthermore, the light is spread across the entire array and, although the power per unit area does not increase, the effective aperture is increased by a factor of N . Since increasing the effective aperture by N reduces the divergence by N the radiance is increased N -fold, just as with beam superposition.

Two-Dimensional Semiconductor Laser Arrays

Most previous diode laser beam addition schemes have employed techniques suited to one-dimensional laser arrays [2]. Two-dimensional arrays may achieve power densities of several hundred watts per square centimeter across the entire array. Consequently, they are prime candidates for beam combining. Surface-emitting geometries [3-6] offer the high reliability and mass-fabrication potential of a monolithic structure, coupled with efficient heat removal. The goal of our work has been to develop laser beam addition techniques matched to the characteristics of two-dimensional arrays.

We have performed several laser addition experiments using methods applicable to two-dimensional laser arrays. The following sections describe three different experimental

configurations for establishing coherence, phasing the lasers, and combining the beams. The role of the binary-optical elements will be described for each of these configurations.

We begin by describing a laser beam addition system based on the method of beam superposition. We then consider two systems based on different approaches to aperture filling. Finally, the benefits and limitations of each system are described and appropriate applications discussed.

Superposition of Laser Beams Using Binary Phase Gratings

Laser beam superposition can be accomplished using a specially designed diffraction grating. The laser beams are made to cross each other at a given point, resulting in an interference pattern $|E(x,y)| \exp [j \phi(x,y)]$ that is dependent on the beam angles and the relative phases of the lasers. The grating is placed in the interference plane to convert the field into a single beam. For perfect conversion into an apertured plane wave, the highly collimated, low-divergence wave we seek, the grating should have a transmittance equal to the reciprocal of the interference, or

$$t(x,y) = \frac{1}{|E(x,y)|} \exp [-j\phi(x,y)] . \quad (1)$$

The amplitude transmittance of the grating is restricted to values less than or equal to one. Since any absorption results in an undesirable loss of laser power, the amplitude transmittance is chosen to be unity, and the amplitude component of the interference pattern is not changed. The phase term, however, can be corrected by constructing a grating with the phase of Eq. 1. After passing through this conjugate phase grating, the light amplitude coupled into the zero-order beam is given by the average of the resultant field

$$A_0 = \int_{-\infty}^{\infty} \int_{-\infty}^{\infty} |E(x,y)| dx dy . \quad (2)$$

The grating coupling efficiency is maximized by choosing laser phases that produce an

interference amplitude $|E(x,y)|$ to maximize Eq. 2. The coupling of six lasers, for example, is maximized using laser phases of $(\pi, \pi, 0, 0, \pi, \pi)$; the resulting coupling efficiency from Eq. 2 is 81% [7].

Establishing Coherence

The common-cavity configuration of Fig. 1 is used to establish coherence and proper phasing between lasers. The output mirrors from each laser are replaced by a single common output mirror. The binary grating inside the cavity couples the laser beams into a single output beam. Any loss of coherence or change in relative laser phases results in lower coupling into the on-axis order and correspondingly diminished feedback. The lowest threshold lasing condition occurs when the lasers are both coherent and in the correct phase state for efficient beam combination.

In addition to combining the beam, diffraction gratings designed to operate inside a common cavity must distribute the single feedback beam *equally* among the lasers with a minimum of loss to higher orders. A phase grating with the phase transmittance of Eq. 1 does not necessarily have

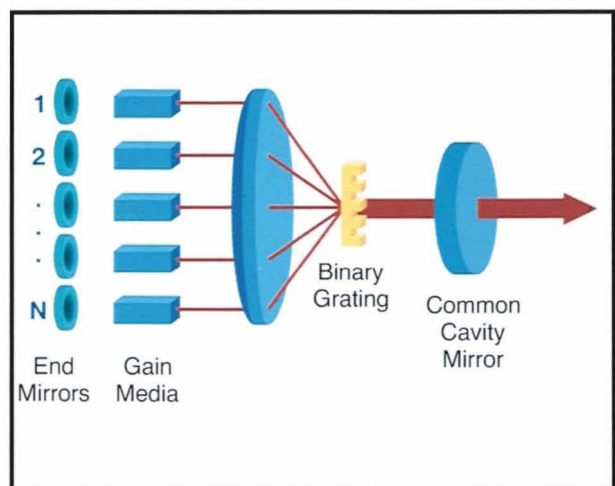


Fig. 1 — The common-cavity configuration establishes mutual coherence by obtaining the feedback light from a common output mirror shared by all the lasers.

this property. By careful modification of the phase transmittance, we can design a grating to split a single beam into N equal-intensity beams with maximum efficiency. This splitting efficiency is identical to the efficiency of combining the N beams into a single beam with the same grating. (See the box, "Binary Gratings for Splitting and Combining Laser Beams.") Thus, the gratings can simply be designed to have good beam-splitting properties, and the combination properties follow automatically.

Binary phase-only structures have been studied previously for splitting a laser beam into N equal orders [8]. In these studies, classical optimization methods were applied to select the best grating shape. Our approach has been to employ least-squares iterative techniques to adjust the grating profile until the diffraction pattern is optimized to the desired shape.

Experiments

A binary phase grating designed to couple six lasers was fabricated in a quartz substrate [9]. This grating was placed in the common-cavity configuration of Fig. 1. Six lasers from an antireflection-coated AlGaAs diode array were positioned along the ± 1 , ± 2 , and ± 3 diffraction orders of the grating. The coherence and phase relationships between the sources were measured by interfering pairs of sources together and observing the interference pattern. The resulting stable sinusoidal patterns indicated that the lasers were indeed coherent with respect to one another, and that the phase relationship between lasers was $(\pi, \pi, 0, 0, \pi, \pi)$, as expected. The light distribution in the various grating lobes is shown in Fig. 2 (a). The one large on-axis order contains 68.4% of the energy from the six lasers. The far-field output of the six combined laser beams is compared with a single laser (scaled in intensity) in Fig. 2 (b). The two far fields are almost identical since the six laser sources are coherently superimposed onto one another, producing a beam with the divergence properties of a single source.

The grating superposition technique has been applied to a variety of additional laser systems. Three high-gain HeNe laser amplifiers operating

at a wavelength of $3.39 \mu\text{m}$ were placed in the configuration of Fig. 1. Piezoelectrically controlled end mirrors were provided for each gain tube, and a common-output coupler was placed after the binary grating. The grating was used in reflection by applying a gold coating to the etched quartz substrate. The end mirrors

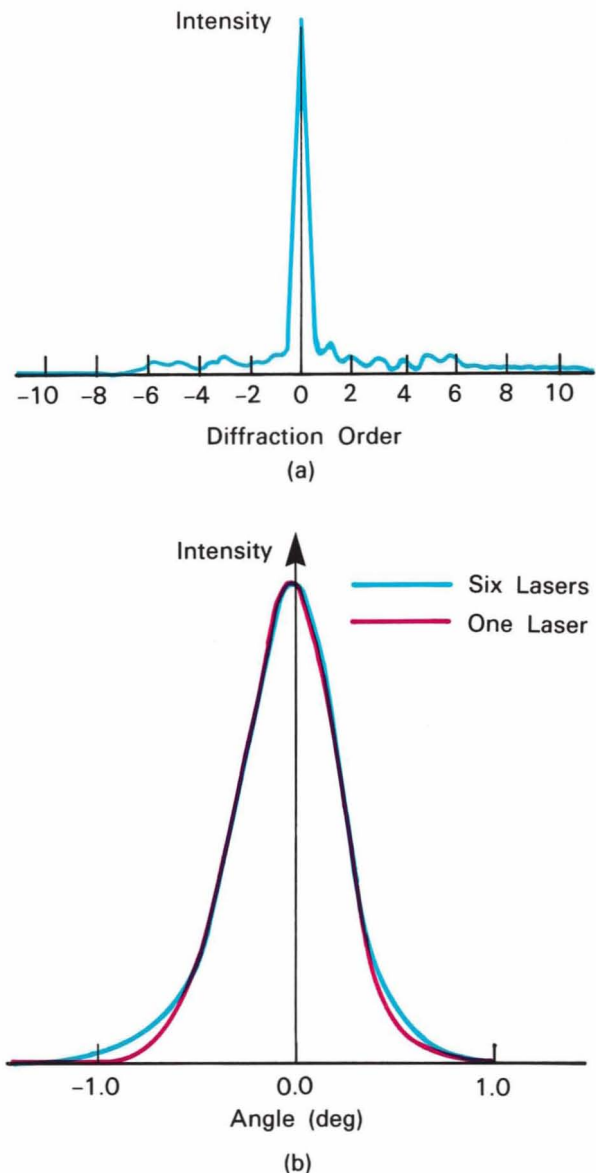


Fig. 2 — Six lasers were combined by superposition to obtain the angular plane-wave spectrum of light shown in (a). 68.4% of the energy is contained in the on-axis lobe. The far-field output of the combined lasers is nearly identical to that of a single laser, as shown in (b). The outputs are scaled in intensity for comparison.

Binary Gratings for Splitting and Combining Laser Beams

The superposition of N laser beams is accomplished by a specially designed diffraction grating. The transmittance of the grating can be expressed as a Fourier series with each term of the series corresponding to a grating diffraction order [1]

$$t(x) = \sum_{n=-\infty}^{\infty} a_n \exp(j\phi_n) \exp(jn\alpha x), \quad (4)$$

where a_n and ϕ_n are the magnitude and the phase of the n th plane-wave component and α is proportional to the sine of the angle between diffraction orders. (N is assumed to be even in this derivation, and one-dimensional notation is used for simplicity.) The grating splitting efficiency ζ is defined as the amount of power contained in the $N+1$ largest orders compared with the total incident power

$$\zeta = \sum_{n=-N/2}^{N/2} a_n^2. \quad (5)$$

Coherent addition of laser beams can be accomplished by operating this grating in reverse. The grating is illuminated with

$N+1$ laser beams at angles corresponding to the original grating diffraction orders. The laser beams have amplitudes a_m equal to the original diffraction-order amplitudes and their phases are chosen to be the complex conjugates of the diffraction orders. The interference pattern of these beams in the plane of the grating is then given by

$$E(x) = \sum_{m=-N/2}^{N/2} a_m \exp(-j\phi_m) \exp(-jm\alpha x), \quad (6)$$

where the Gaussian profile of the laser is unimportant to the derivation and is not included.

The amplitude of the light after passing through the grating is given by the product of Eqs. 4 and 6. The cross terms that result represent all the plane waves leaving the grating. The on-axis plane waves correspond to the terms where $m = n$. The power in the zeroth diffraction order of the grating is given by the square of the coherent sum of these on-axis plane waves

$$P_0 = \left[\sum_{n=-N/2}^{N/2} a_n^2 \right]^2. \quad (7)$$

The efficiency η of coupling the power from the $N+1$ laser beams into the central order can be defined as the ratio of the zero-order grating power to the incident power. Since the $N+1$ lasers have an incident power of

$$P_i = \sum_{n=-N/2}^{N/2} a_n^2, \quad (8)$$

this ratio is given by

$$\eta = \frac{\left[\sum_{n=-N/2}^{N/2} a_n^2 \right]^2}{\sum_{n=-N/2}^{N/2} a_n^2} = \sum_{n=-N/2}^{N/2} a_n^2 = \zeta. \quad (9)$$

Since the coupling efficiency η and the splitting efficiency ζ are identical, highly efficient beam superposition gratings can be designed by maximizing the grating splitting efficiency.

Reference

1. W.B. Veldkamp, J.R. Leger, and G.J. Swanson, "Coherent Summation of Laser Beams Using Binary Phase Gratings," *Opt. Lett.* **11**, 303 (1986).

were adjusted to change the cavity lengths, thereby satisfying the phase condition necessary for good phase locking and highly efficient beam combining. Similar experiments were conducted on CO₂ waveguide lasers and Nd: YAG ring lasers both within our group and at other laboratories [10].

The grating superposition technique can be used to combine lasers that have been properly

phased and made mutually coherent through other means. An injection-locked configuration is shown in Fig. 3. The master oscillator signal applied to each laser serves to lock the outputs to a common source, thereby establishing coherence across the array. In this scheme, the grating serves the dual purpose of distributing the injection-locking signal uniformly among the N slave lasers as well as combining their

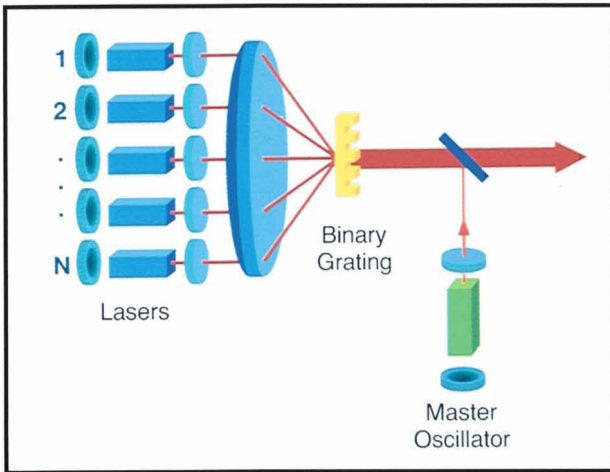


Fig. 3 — Coherence is established by injection-locking each laser to a single master oscillator. The grating both combines the lasers into a single beam and distributes the master oscillator signal.

outputs into a single beam.

Although the method of grating superposition was applied both to gas and semiconductor laser sources, it appears to be most appropriate for low-divergence sources that don't require additional collimation of the laser beams. The next section describes the second method of beam combining, based on the technique of aperture filling.

Aperture Filling by Amplitude-to-Phase Conversion

The method of aperture filling combines laser beams by spreading light uniformly across the entire laser array. Perfect aperture filling results in a light distribution that is uniform in amplitude and phase. Amplitude-to-phase conversion (APC) employs binary-optical elements for spatial filtering and phase correction to approximate a uniform light distribution.

As we have seen, techniques for increasing laser radiance require mutual coherence across the laser array. In the previous section, this coherence was established by an external cavity. In this section, we assume that the coherence is provided by the design of the array itself. Both Y-guide and evanescently coupled

semiconductor laser arrays are examples of such configurations. When the array is designed to force the emitters to radiate in-phase, the phase component of the resultant electric field is constant across the array. The amplitude component is nonuniform, however, because of the separation of the individual lasers and their Gaussian mode structure. It is this amplitude variation of the light across the output aperture that gives rise to the undesired off-axis grating lobes in the far field. The percentage of power left in the central grating lobe is approximately equal to the array fill factor, or the percentage of the laser array covered by the lasing apertures.

The APC technique performs a field transformation on the complex amplitude of a phase-locked laser array by spatially filtering the on-axis grating lobe with a phase filter. The result of this transformation is an electric field that is nearly uniform in amplitude and varies in phase. (See the box, "Amplitude-to-Phase Conversion.") The far-field intensity of the transformed field is identical to the original far field, but the grating lobes are now caused by phase variations rather than amplitude variations in the light. These phase variations can be eliminated with a phase-correcting plate. The result is a light distribution that is nearly uniform in both amplitude and phase. The far-field pattern, therefore, concentrates virtually all its energy in the desired central lobe. Since the optical elements are phase-only, no light is lost in the process of beam combination.

In theory, 100% of the light from an ideal array can be coupled into the central grating lobe. The performance of the technique on a real array is limited by four factors: I. Arrays with fill factors less than 25% result in incomplete aperture filling and reduced coupling efficiency. II. The mode profile of an individual laser in a real array is Gaussian, rather than rectangular; this introduces a residual amplitude ripple in the result. III. Ideally, the phase corrector used with a Gaussian-shaped beam should be continuous, but a binary phase corrector is usually employed. IV. Real laser arrays are finite in extent; consequently, it is impossible to separate completely the on-axis lobe from the higher-order grating lobes during the

amplitude-to-phase transformation. In spite of these restrictions, computer simulations indicate that coupling efficiencies of greater than 95% are achievable using APC.

Figure 4 illustrates the optical configuration required for implementing the APC technique. A laser array is placed in the front focal plane of an afocal imaging system consisting of two lenses. An amplitude-to-phase transformation is produced by placing a phase filter in the back focal plane of the first lens. The filter consists simply of a phase-shifting spot designed to cover the central grating lobe of the array, where the amount of phase shift is chosen to minimize the amplitude variations in the image plane (back focal plane of the second lens). The phase variation in the image plane is canceled by the binary phase correction plate, resulting in an approximately uniform plane wave.

Experiments

The APC technique was tested on a phase-locked CO₂ ridged-waveguide array in collaboration with Leon Newman and his group [11, 12]. An all-reflective imaging system insured high-power density handling capability and its folded configuration with 15-cm focal length offered modest size. Its compactness allowed it to be directly attached to the laser head. For the case of the 35-W dual-waveguide array of Ref. 13, the percentage of power in the central far-field lobe was increased from 71% to 94%. Application of the technique to phase-locking an uncoupled CO₂ waveguide array (five channels) in an external cavity was also demonstrated [11].

Aperture filling was also performed on a coupled 10-element AlGaAs Y-guide laser array.

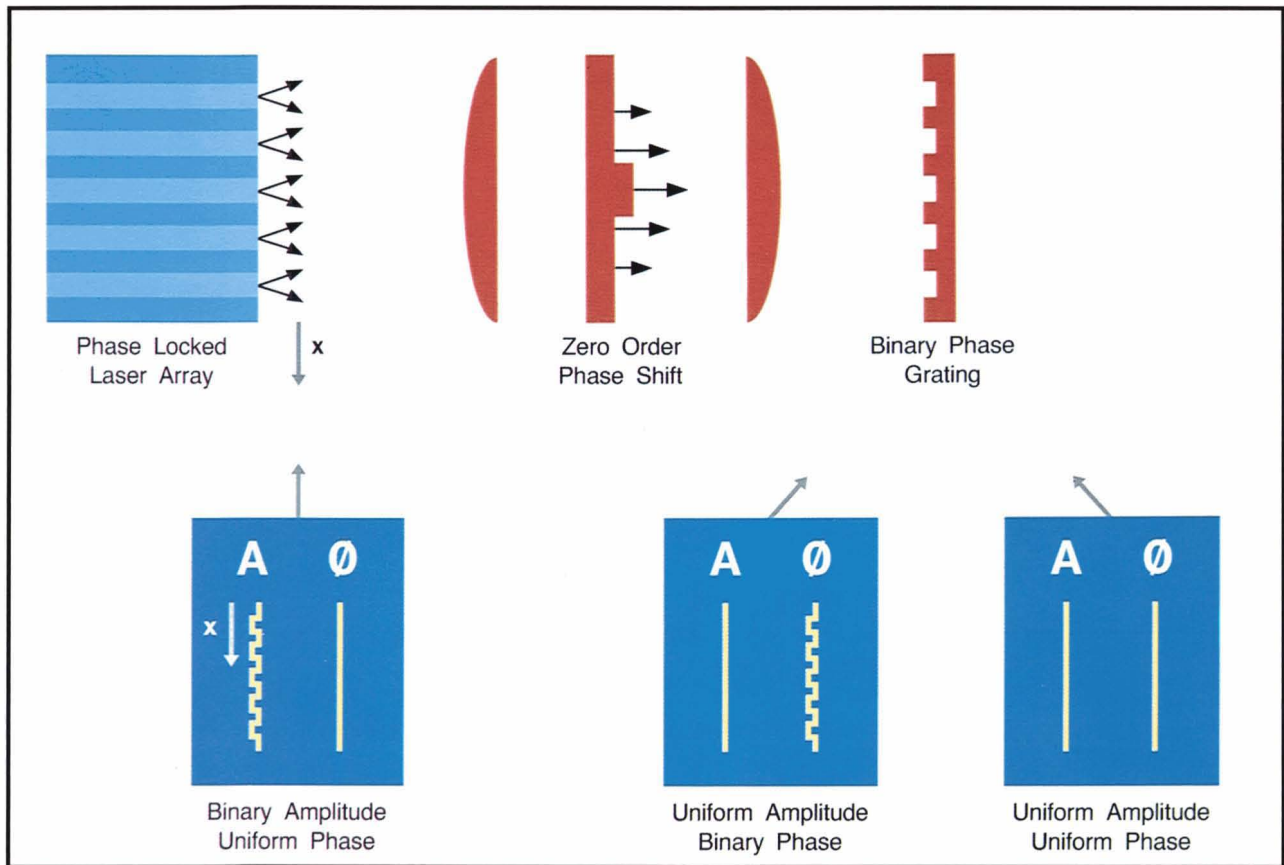


Fig. 4 — An idealized laser array produces a light field with a nonuniform amplitude but uniform phase. The lenses and phase shifter convert this into a uniform amplitude and varying phase. The phase grating corrects for the residual phase variation.

Amplitude-to-Phase Conversion

The field transformation required to perform amplitude-to-phase aperture filling can be understood by expressing the complex light field as a phasor in the complex plane. Figure A (left) shows an idealized amplitude and phase distribution from a laser array. The amplitude has a value of unity over the lasing apertures and zero elsewhere. The phase is assumed to be uniform over the entire aperture. These two complex values are plotted as two points in the phasor diagram. The two points can be represented as the sum of two phasors. The unity value is given by a constant phasor (dc) plus a positive-going phasor. The zero value is given by the same constant phasor plus a negative-going phasor. If we shift the phase of the constant phasor by 90° , the diagram in Fig. A

(right) results. The phasor sums now have equal amplitude (length of phasor sum) and different phases (direction of phasor sum). The phase variation can be canceled out by a subsequent phase-correcting optical element to produce a field with constant amplitude and constant phase.

Aperture filling was first demonstrated using a coherently illuminated amplitude mask [1] to simulate a phase-locked array with a fill factor of 25%. The central-lobe phase spot and the binary phase corrector were constructed by etching the proper patterns into quartz substrates. The results of this experiment are shown in Fig. B. The upper left is a photograph of the output aperture of the simulated array with a fill factor of 25%. The upper right shows the resulting far-field

pattern of the unmodified array consisting of a central lobe containing 25% of the power and several higher-order grating lobes. The lower left is a photograph of the irradiance distribution of the modified field at the binary phase corrector plane. Light initially existing over only 25% of the aperture has been redistributed to fill the entire aperture. The far-field irradiance of the field emitted from the binary phase corrector is shown in the lower right. The central lobe of this pattern contains 92% of the total measured power.

Reference

1. G.J. Swanson, J.R. Leger, and M. Holz, "Aperture Filling of Phase-Locked Laser Arrays," *Opt. Lett.* **12**, 245 (1987).

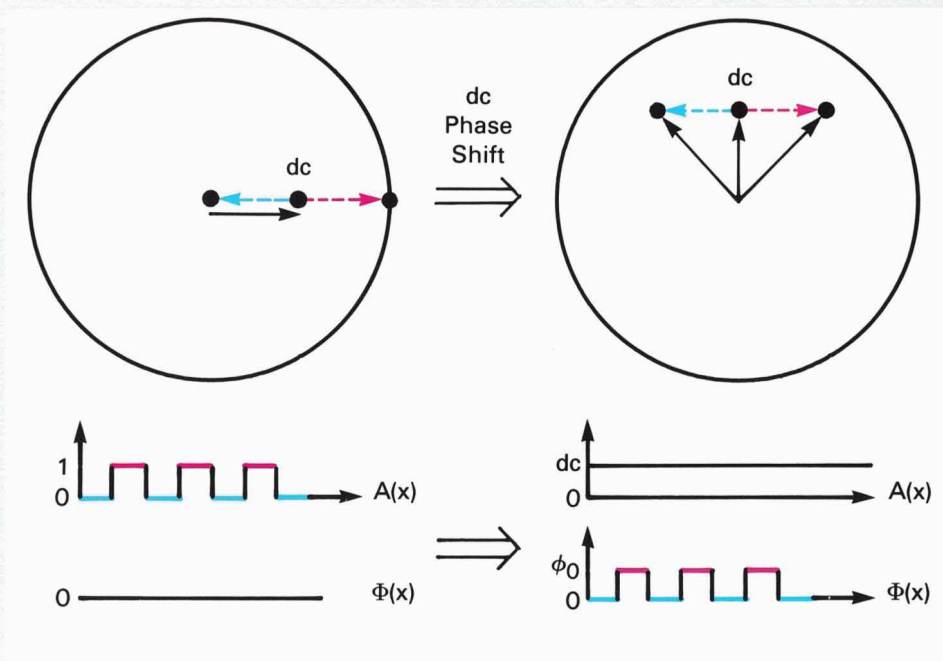


Fig. A — The phasor diagram on the left corresponds to a light field with an amplitude variation. Phase-shifting the dc or on-axis component by 90° results in the phasor diagram on the right, showing uniform amplitude and varying phase.

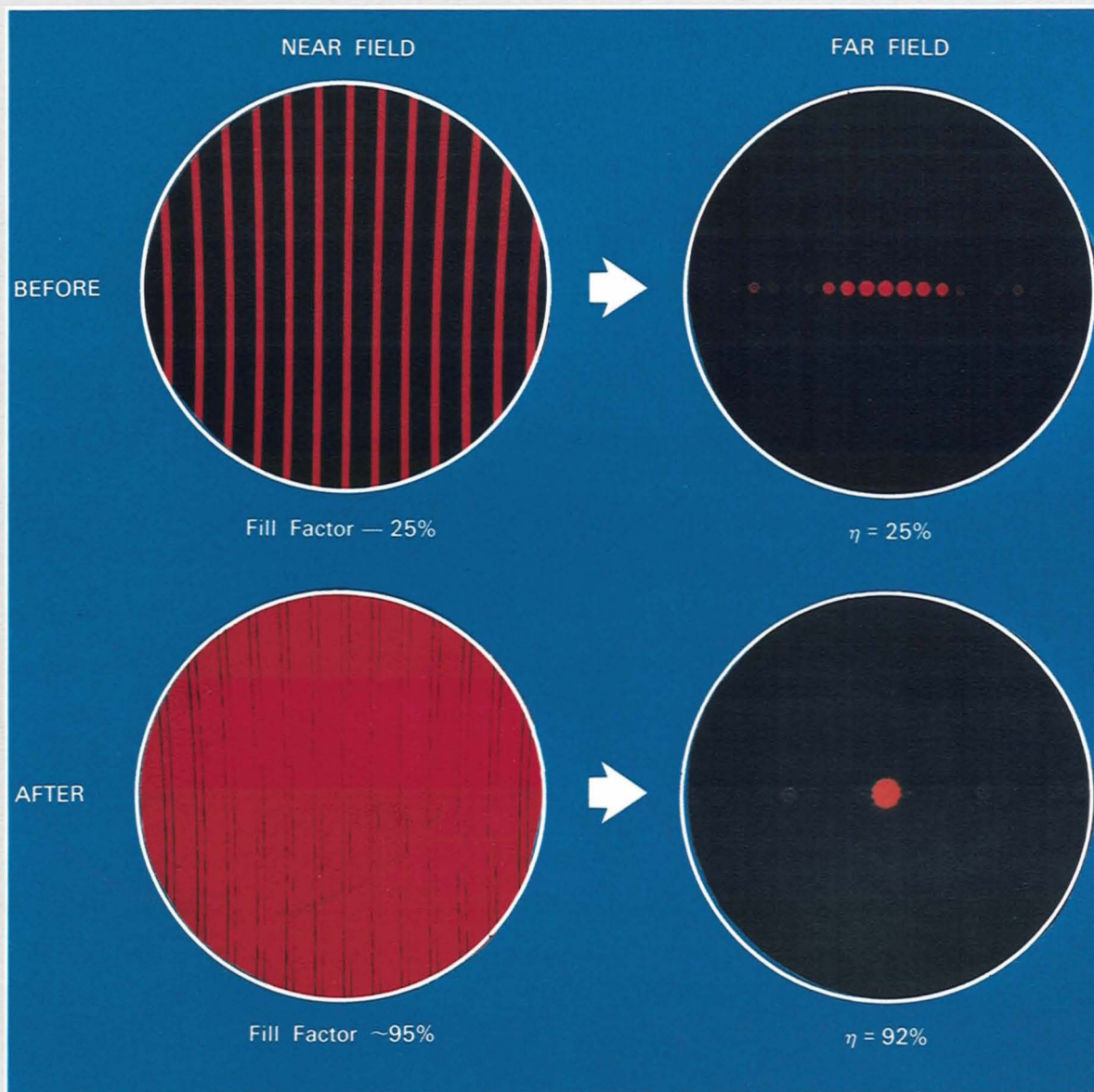


Fig. B— A simulation of a laser array with a 25% fill factor shows a far field with several grating lobes. Aperture filling increases the content of the central lobe from 25% to 92%.

Figure 5 shows the experimental results from an array consisting of 2.4- μm laser apertures spaced by 6.0 μm [14]. The Y-patterned waveguide configuration established coherence across the array and ensured that the lasing apertures were all in phase [15]. Figure 5 (a) shows the far-field pattern before aperture filling. Three distinct grating lobes can be seen, with only 51% of the power contained in the central lobe. Figure 5 (b) shows the result of aperture filling. The off-axis grating lobes are almost entirely eliminated, and their power has

been deposited in the main lobe. The intensity in the center of the main lobe has almost been doubled, with the entire main lobe containing 90% of the total power produced by the array.

Sidelobe suppression of a 40-stripe evanescently coupled AlGaAs array is shown in Fig. 6. The array operates in the out-of-phase mode (top trace in Fig. 6), which we converted to the in-phase mode by use of a suitable phase corrector (middle trace in Fig. 6). The effect of aperture filling is shown in the bottom trace. In contrast to beam superposition, the aperture-

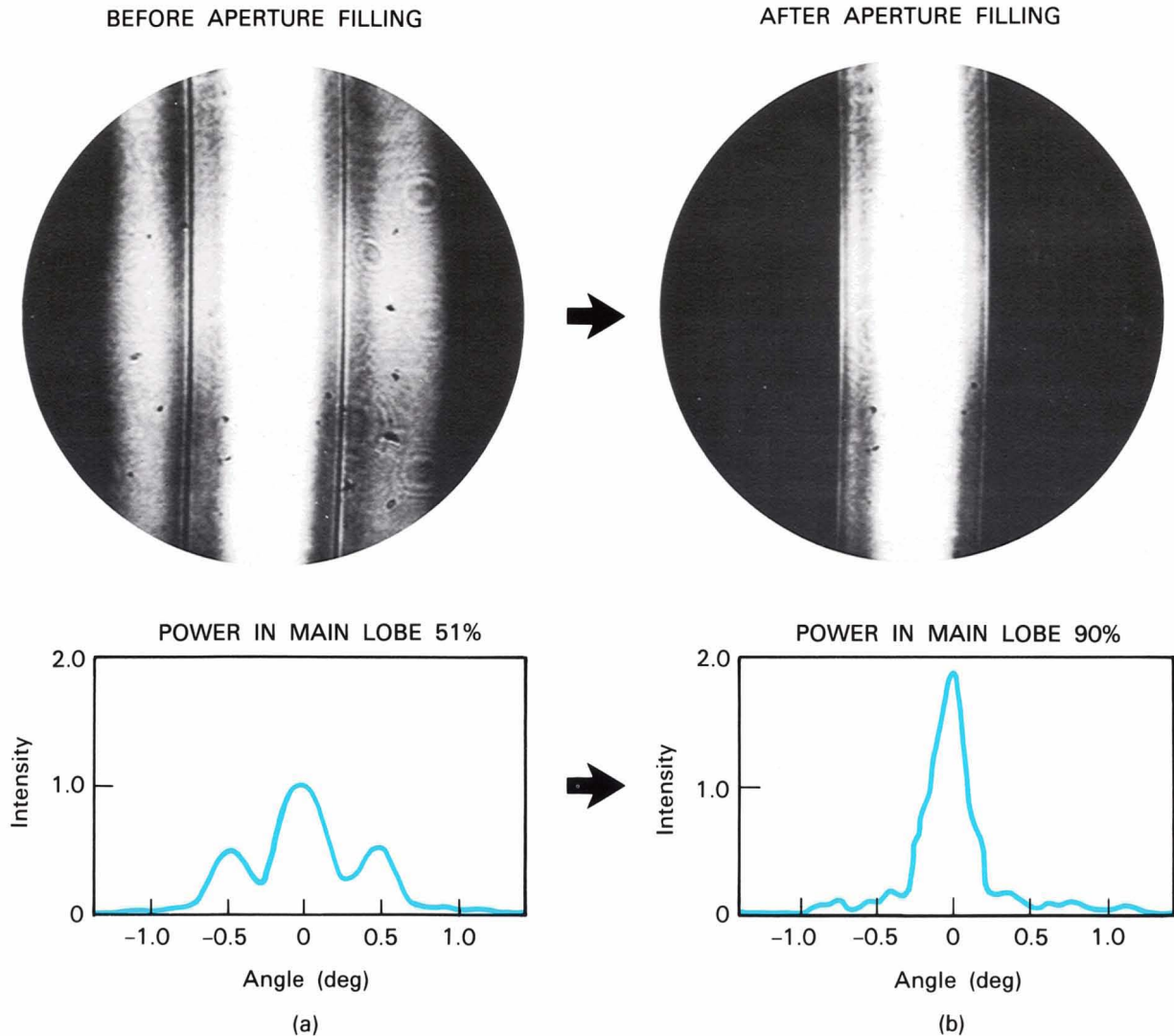


Fig. 5 — (a) Far-field intensity distribution of a 10-element AlGaAs array before aperture filling. The central lobe contains only 51% of the power. (b) Improvement afforded by aperture filling: 90% of the power is in the central lobe.

expands in a cone of 20° to 30° . After a few hundred microns of propagation, the cones of light from adjacent lasers intersect. Collimating each laser beam at this point produces a wavefront with the desired uniform phase and quasi-uniform intensity.

Although the collimation can be performed in principle using a lens for each laser, the lens requirements are quite strict. The size of each lens must be equal to the inter-laser spacing of the array: typically between ten microns and several hundred microns. In order to prevent gaps in the resulting wavefront, each lens must be placed as close to its neighbor as possible. The lenses must have a low f -number to collect the laser light efficiently. Rectangular lens apertures are required to allow the f -numbers of each lens to be optimized along the horizontal and vertical axes. Diffractive and absorptive losses must be kept to a minimum. In addition to having low intrinsic aberration, each lens must correct for any aberrations in the original laser beam in order to produce an aberration-free collimated beam.

We have found that diffractive microlenses can be designed to satisfy each of these requirements [16]. The microlenses are produced utilizing the binary-optics techniques previously described. (See the box, "What Is Binary Optics?") These methods have the flexibility and precision required to produce lenslet patterns of virtually any size and shape. In addition, large arrays of accurately spaced lens patterns can be fabricated. Advanced lithographic and etching techniques transfer these patterns into a quartz substrate with the submicron accuracy required for high-speed $f/1$ lenses.

Simple diffractive lenses produced by a single etching step focus 40.5% of the available power into the desired focal spot. We have developed techniques to increase the diffraction efficiency by performing multiple etches. The resulting multilevel lens can have a diffraction efficiency approaching 100%. Figure 7 is a scanning-electron micrograph of microlenses made by this technique. A two-step etch was performed, resulting in four discrete etch levels. The theoretical diffraction efficiency of this lens is

81%. The lens spacing is $50\ \mu\text{m}$, corresponding to the spacing of the lasers in the matching array. The shape of each lens is rectangular, resulting in an $f/1$ lens in one direction and an $f/2$ lens in the other. The lenses were also designed to correct for an astigmatic aberration present in the original laser beams. The elliptically shaped patterns result in an anamorphic lens with a focal length of $100\ \mu\text{m}$ parallel to the array and $69\ \mu\text{m}$ perpendicular to it.

Our diffractive lenses have shown excellent optical performance. Diffraction efficiencies as high as 93% have been measured from eight-level lenses produced by three successive etching steps. The wavefront quality of an $f/2$ microlens with a $100\text{-}\mu\text{m}$ focal length was measured using a WYKO interferometer, and is displayed in Fig. 8 (a). The flatness of the wavefront corresponds to an rms phase error of $\lambda/50$. The modulation transfer function in Fig. 8 (b) shows near diffraction-limited performance, with a Strehl ratio of 0.98 (a Strehl ratio of 1.0 indicates diffraction-limited performance).

Coupling Microcavities by Talbot Self-Imaging

In 1836, W.H.F. Talbot reported several interesting observations regarding diffraction from periodic objects [17]. He discovered that illuminating a periodic object with coherent

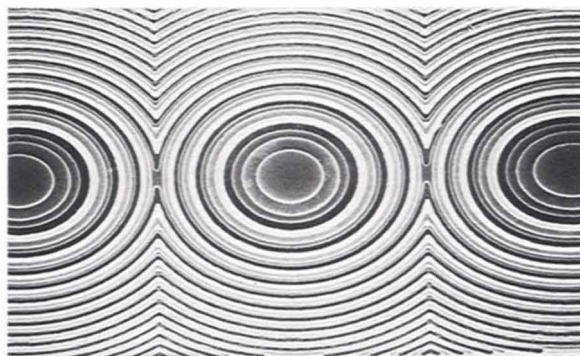


Fig. 7 — Two etches produced this array of four-level microlenses spaced $50\ \mu\text{m}$ apart. The theoretical diffraction efficiency of this lens is 81%.

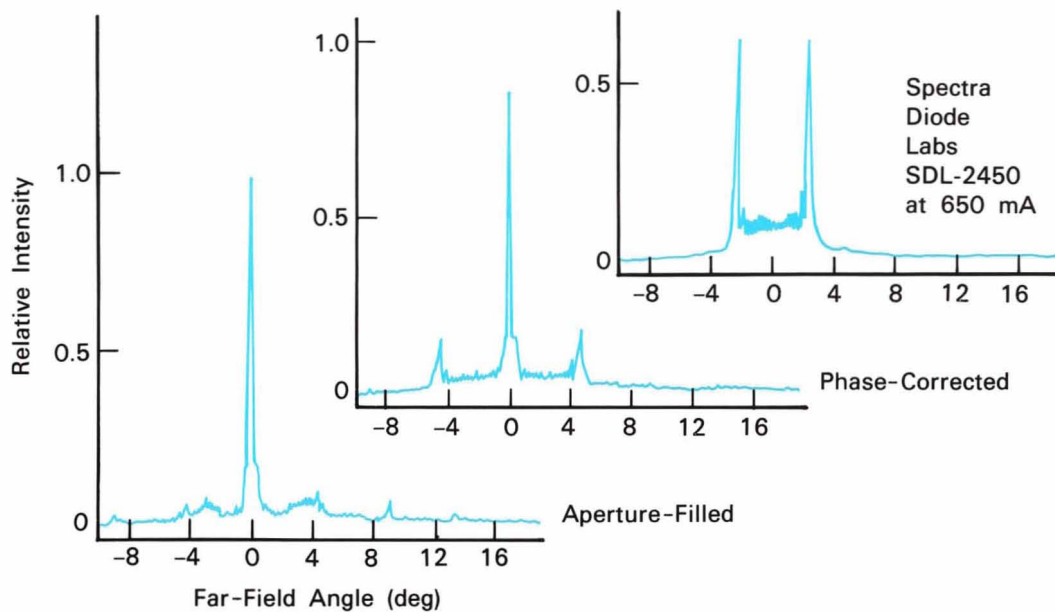


Fig. 6 — The power of a 40-stripe evanescently coupled array is distributed nearly evenly in the first two grating lobes (top). After phase correction and aperture filling, most of the power is contained in the central lobe.

filling technique results in a diffraction-limited far-field beam that is inversely proportional to the transverse dimension of the laser array rather than to an individual laser. Therefore, smaller diffraction spots and lower beam divergence are achievable without recourse to additional beam-expanding optical elements.

Several extensions of the present technique are possible. The method can be cascaded by applying the output of the present system to the input of a new system. Virtually 100% of the power can be transferred to the main lobe for a large variety of laser-array fill factors and light distributions. Coated optics can ensure that the optical train introduces negligible loss. The technique can also be applied to side-lobe suppression of phased arrays of lasers for beam-steering applications. It can be applied to other laser systems and different methods of establishing array coherence. Finally, the method is directly extendable to two-dimensional arrays of lasers, with the proviso that the arrays have a fill factor greater than 25%. For arrays with fill factors less than 25%, the coupled microcavity approach can provide the aperture filling needed for coherent addition of lasers.

Aperture Filling by Coupled Microcavities

Coupled microcavities (CMC) provide a third method of laser beam addition. In this approach, diffractive microlens technology and the unique properties of Fresnel diffraction are used to create an array of small coupled laser cavities. The coupling locks the laser cavities together in a coherent ensemble and produces a narrow-beam far-field pattern. The diffractive microlenses distribute the laser light uniformly across the array, thereby producing a filled aperture that channels the light into the central lobe of the far field. The flexibility of binary microlens technology makes it particularly well-suited to the addition of large two-dimensional laser-diode arrays.

The previous aperture-filling technique employed a spatial filtering system to spread the light from the individual lasers in an array across the entire array aperture. The phase of this light field was later corrected by a grating. An alternative way of spreading the light is through diffraction. Since the lasing aperture of a semiconductor laser is small its divergence is very high; the light from a typical laser beam

light produces an image at regular intervals by free-space diffraction alone. This self-imaging property, now known as the Talbot effect, is illustrated in Fig. 9 (top) (pg 242). It wasn't until the end of the nineteenth century that Lord Rayleigh [18] provided an explanation for the phenomenon and deduced the distance between the self-image planes. (See the box, "The Talbot Effect.") Since then, the effect has been employed only sporadically in the design of optical instruments [19, 20].

Although the diffraction pattern of the entire array has self-imaging properties, the diffracted light from a single element continues to expand with increasing distance. Figure 9 (top) shows that the light from the single element in red actually contributes to several elements in the first self-image. This property is combined with Talbot imaging of the entire array to form a Talbot cavity shown in Fig. 9 (bottom). An external optical cavity is created by placing a flat output mirror a short distance behind an array of antireflection-coated lasers. Light from a single laser reflects off the output mirror and back to the laser array to form a microcavity. This individual feedback beam spreads by diffraction to extend over several lasers, providing the optical coupling needed for mutual coherence. By positioning the output mirror so that one cavity round trip corresponds to a Talbot distance, the free-space diffraction from the entire laser array produces a self-image of the original laser apertures. This ensures that the light will couple efficiently into the individual laser waveguides. If the lasing apertures are not mutually coherent, the Talbot effect no longer applies and no self-image is formed. Much of the light falls between laser apertures and is lost. The lower loss and subsequent higher efficiency of the mutually coherent state acts to ensure coherent operation.

Experiments

Experiments have been performed in our laboratory using a linear array of AlGaAs laser diodes [21]. The array was custom-fabricated by Spectra Diode Laboratories with the front laser facets coated for minimum reflectivity. The laser

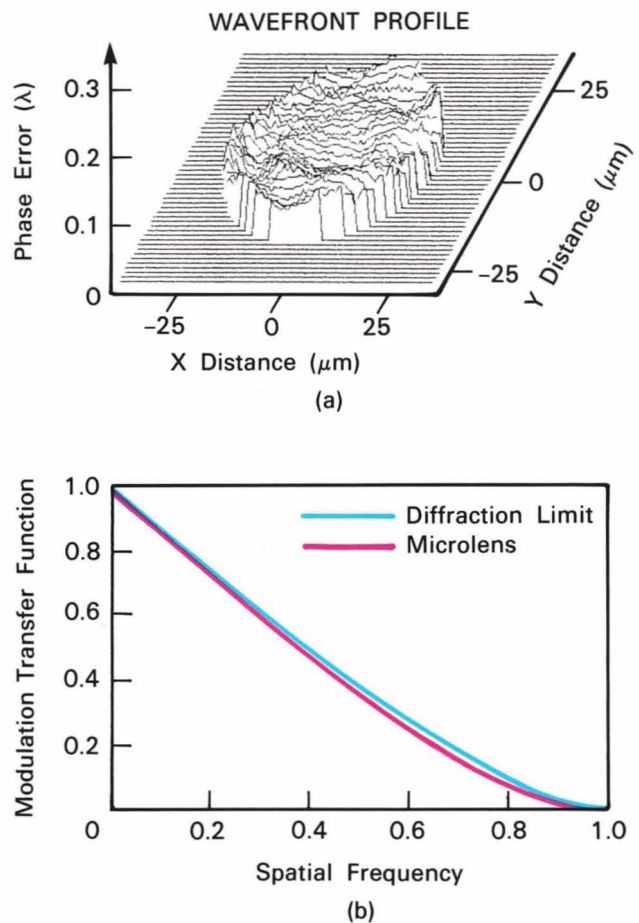


Fig. 8 — (a) The wavefront from an $f/2$ microlens exhibits a flatness corresponding to an rms phase error of $\lambda/50$. (b) The modulation transfer function shows near diffraction-limited performance.

separation was chosen as $50 \mu\text{m}$ to eliminate evanescent coupling. Figure 10 (pg 242) shows the experimental setup. The lasers were collimated by a microlens array, and a Talbot cavity was formed by placing a flat output mirror $1/2$ Talbot distance from the microlenses.

The far-field pattern from six laser diodes is shown in Fig. 11. With the output mirror positioned 3 mm behind the lenslet array to satisfy the Talbot imaging condition, the lasers locked together in phase and formed a coherent ensemble. The far-field pattern of Fig. 11 sharpened to a near diffraction-limited spike, with 85% of the energy contained in the central lobe. A spectral analysis of the lasers showed lasing at a common wavelength, and

The Talbot Effect

The Talbot self-imaging effect [1] is a consequence of the periodic nature of the coherently illuminated object. Because of this periodicity, the object light field can be expressed as a Fourier series

$$A(x,z = 0) = \sum_{m=-\infty}^{\infty} a_m \exp(j2\pi \frac{mx}{d}), \quad (10)$$

where d is the repetition period of the object, and a one-dimensional analysis is used for simplicity. This expansion corresponds physically to a set of discrete plane waves of complex amplitude a_m . Note that a grating is a simple example of a periodic object, and the discrete plane waves in Eq. 10 correspond to the grating diffraction orders. After propagating a distance z , the m th plane wave is delayed in phase by

$$H(m,z) = \exp(j2\pi \frac{z}{\lambda}) \exp(-j\pi z \lambda \frac{m^2}{d^2}), \quad (11)$$

where λ is the wavelength of light, and the paraxial approximation has been used. The resultant light field then becomes

$$A(x,z) = \exp(j2\pi \frac{z}{\lambda}) \sum_{m=-\infty}^{\infty} a_m \exp(j2\pi \frac{mx}{d}) \exp(-j\pi z \lambda \frac{m^2}{d^2}). \quad (12)$$

It is apparent that when

$$z = 2nd^2/\lambda, \quad n = \text{integer}, \quad (13)$$

apart from an unimportant constant phase, the light field in Eq. 12 is identical to the original light field in Eq. 10, and an image is formed.

The Talbot effect can be

demonstrated quite dramatically by illuminating a periodic array of square apertures with light from a HeNe laser as shown in Fig. A. The diffraction from each aperture causes the geometric shadows of the apertures to blur until they start to overlap. At a distance $z_T = 2d^2/\lambda$ this complex interference pattern produces an image of the original object, seen at the far right in Fig. A. Apart from edge effects from a finite size array, this image will be reproduced periodically at integer multiples of z_T .

Reference

1. J.T. Winthrop and C.R. Worthington, "Theory of Fresnel Images. I. Plane Periodic Objects in Monochromatic Light," *J. Opt. Soc. Am.* **55**, 373 (1965).

measurements of the coherence between two distinct lasers indicated a tightly phase-locked array. On the other hand, with the output mirror placed directly against the lenslet array, no diffractive coupling took place. The lasers were mutually incoherent as a result, exhibiting no phase- or frequency-locking. A spectral analysis of each laser revealed that the wavelengths of the lasers ranged over 20 Å. The far-field pattern consisted of an incoherent superposition of light from each lasing aperture, resulting in a single broad peak.

Coupled microcavities can be applied to a great variety of laser diode arrays. In particular, the beam-shaping and aberration-correction capabilities of microlenses are well-suited to combining large arrays of two-dimensional diode lasers. In addition, coupling the

microcavities by Talbot self-imaging produces efficient coherent operation. The entire system can be contained on a single substrate as illustrated in Fig. 12. The microlens array is etched into the front surface of the substrate, and a partially reflecting output mirror is placed on the back surface. The thickness of the substrate is chosen to satisfy the Talbot self-imaging condition. Future utilization of this technique with large two-dimensional surface-emitting arrays is expected to create many new applications for semiconductor lasers.

Conclusions

Three techniques for laser beam addition have been presented utilizing binary-optic components. Each employs a different method

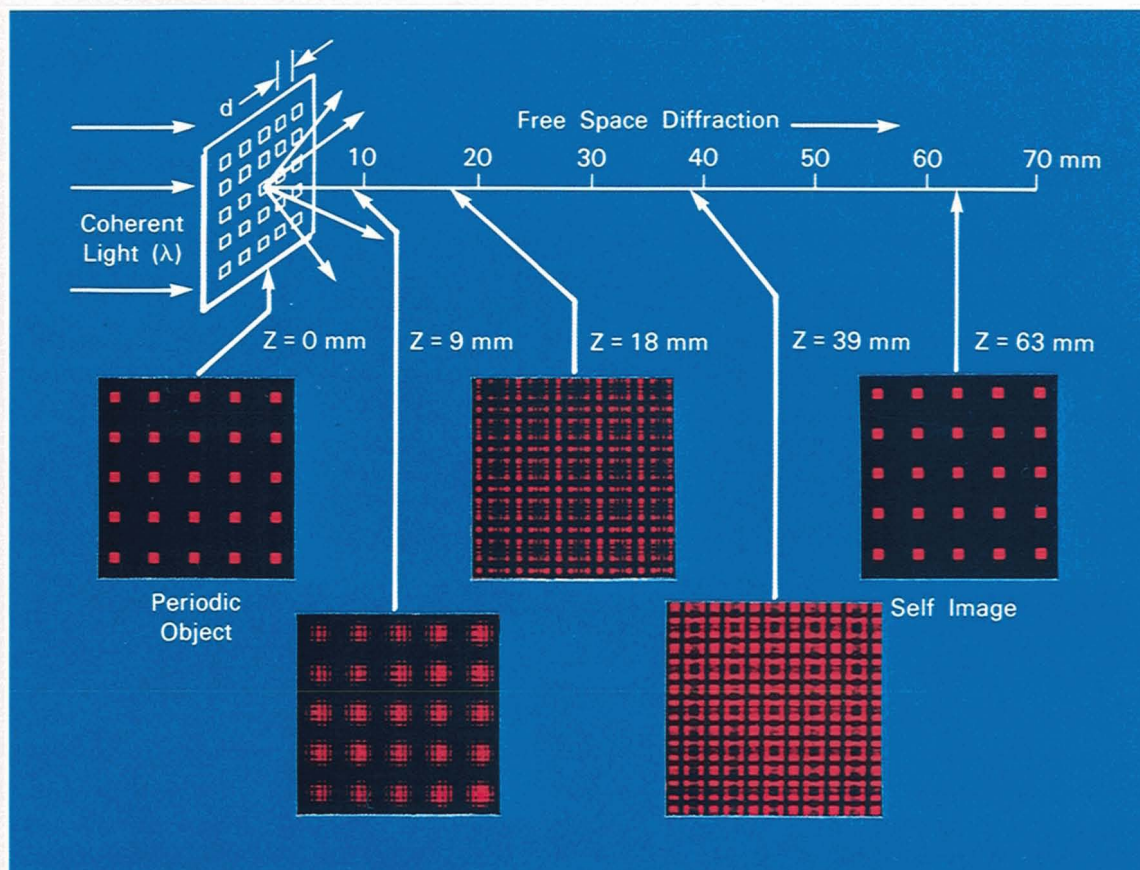


Fig. A — The Talbot effect is illustrated by illuminating a periodic array of square apertures with light from a HeNe laser. A Talbot self-image is formed 63 mm from the object.

for establishing coherence, selecting the proper laser phases, and combining the beams. These techniques can be combined in different ways to create new configurations suited to a particular laser source and application.

One of the key advantages of all the laser addition methods is their immunity to catastrophic failure. Since the approaches are inherently parallel, failure of a single element only reduces the output power slightly. In contrast, linear amplifier chains are susceptible to complete failure if one of the elements in the chain malfunctions. Applications that place a

premium on reliability may benefit from these approaches to beam addition.

The method of beam superposition by gratings is most suited to laser sources with low divergence. These include a variety of gas and solid state lasers such as CO_2 and Nd:YAG. The fill factor of the array is not restricted, and can be very small. The coupling efficiency is limited to 80% to 90% for binary phase gratings, but can be increased to over 90% when a continuous phase grating is used. The technique is expected to find applications in such areas as micromachining, materials processing, and laser radars.

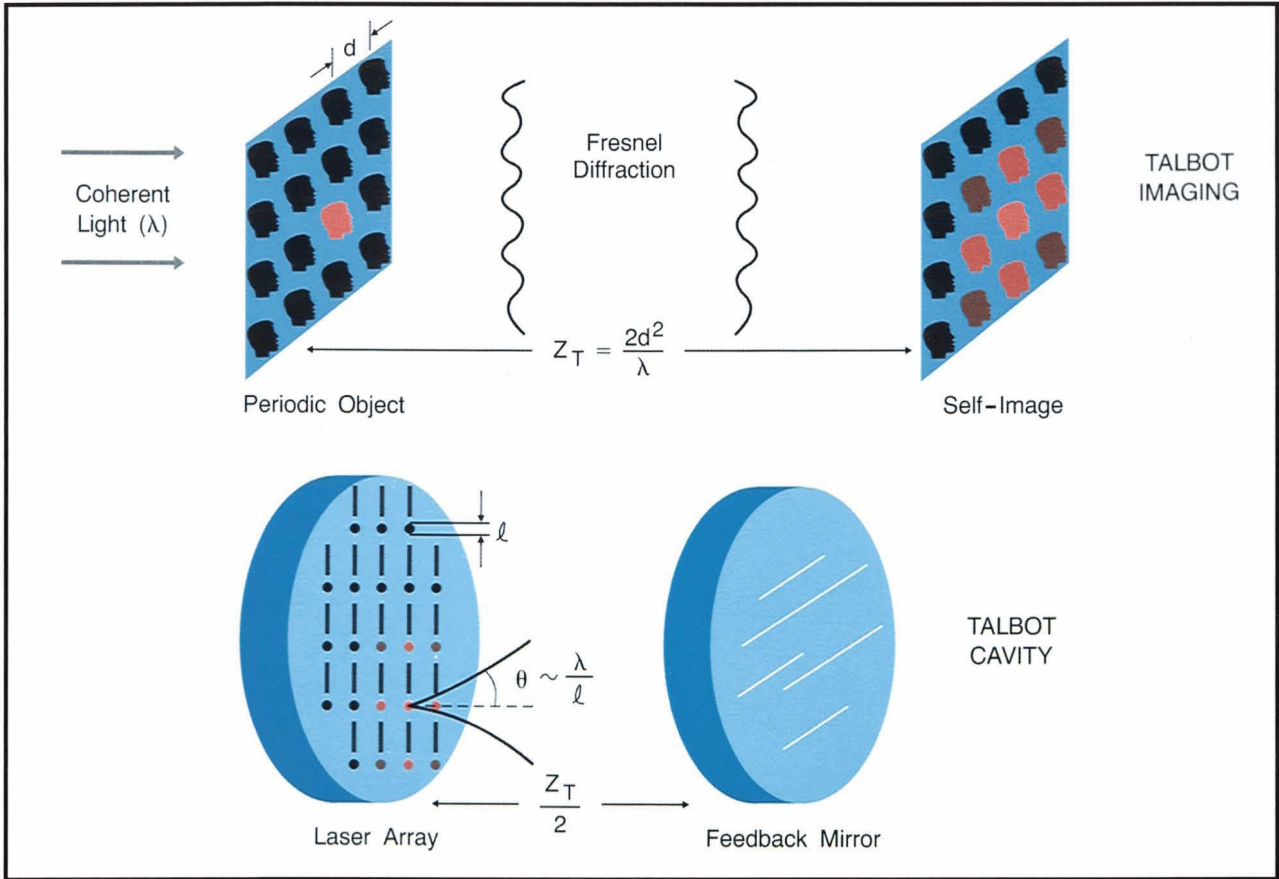


Fig. 9 — Under coherent illumination, light from a periodic object forms a self-image at a Talbot distance. However, light from a single element contributes to several elements in the self-image (top). These two properties are combined to form a Talbot cavity (bottom).

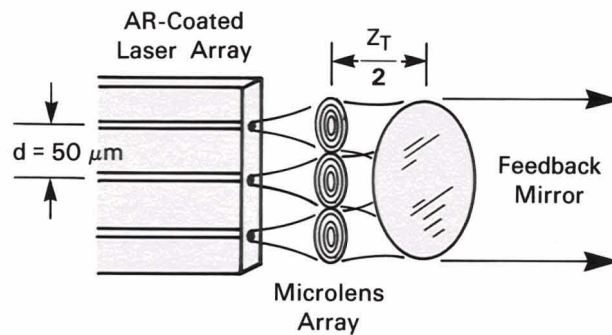


Fig. 10 — In the coupled-microcavity configuration the microlens array is used to collimate the lasers in the array and the output mirror is placed 1/2 Talbot distance from the lenses. The feedback light incident on the lenslet array is a Talbot self-image.

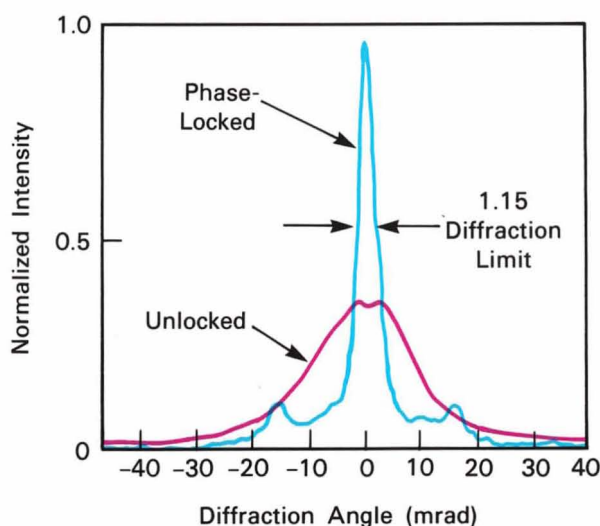


Fig. 11 — This graph illustrates the effectiveness of the microcavity approach. The far-field pattern of six independent lasers is shown for the case where the output mirror is placed against the microlens array (unlocked) and for the case where the mirror is placed at $1/2$ Talbot distance from the microlens array (locked).

The method of aperture filling by APC can be directly applied to a variety of semiconductor laser arrays, where coherence is established by the array design. Many of these laser arrays have the required 25% duty cycle. Another promising application area is coupled CO_2 waveguide lasers. Compact individual waveguide lasers produce as much as 20 W of optical power; coupling even modest arrays of these lasers could produce several hundred watts of optical power. The higher-order grating lobes from these arrays can be virtually eliminated by this method. A key advantage of this technique is its high beam-combining efficiency.

The method of aperture filling by CMC is ideally suited to large two-dimensional semiconductor laser arrays with high divergence and low fill factor. Development of these arrays is being aggressively pursued by many laboratories, and power densities of several hundred watts/cm^2 appear feasible. When the CMC technique is applied to these two-dimensional arrays, exceedingly high

radiance beams are possible. Applications can be anticipated at all power levels. At modest radiance, coherent semiconductor laser arrays can help alleviate the constraints on optical communication systems. The high efficiency and reliability of these sources make them ideally suited to space applications. At higher radiance, these arrays can play an important part in active electrooptic sensors of the future, enabling highly accurate measurements of features such as motion and range. One of the key advantages of the CMC technique is its simplicity and compactness, with the entire optical system contained on a single thin substrate.

This article has concentrated on three specific laser addition systems. We are currently studying the fundamental limits of these techniques, investigating new beam-combination and coherence methods, and applying the various methods to specific applications. We anticipate that this technology will have a significant impact on a wide variety of future electrooptic systems.

Acknowledgments

The experiments described here would not have been possible without the binary-optics devices skillfully fabricated by D. Griswold, P. Bundman, M. Scott, and W. Delaney. We also are grateful for the patient encouragement

and advice of R. Keyes, A. Gschwendtner, and C. Freed. Much of the binary-optics work was made possible by the foresight and support of J. Lupo. For this we thank him.

This work was sponsored by the Defense Advanced Research Projects Agency.

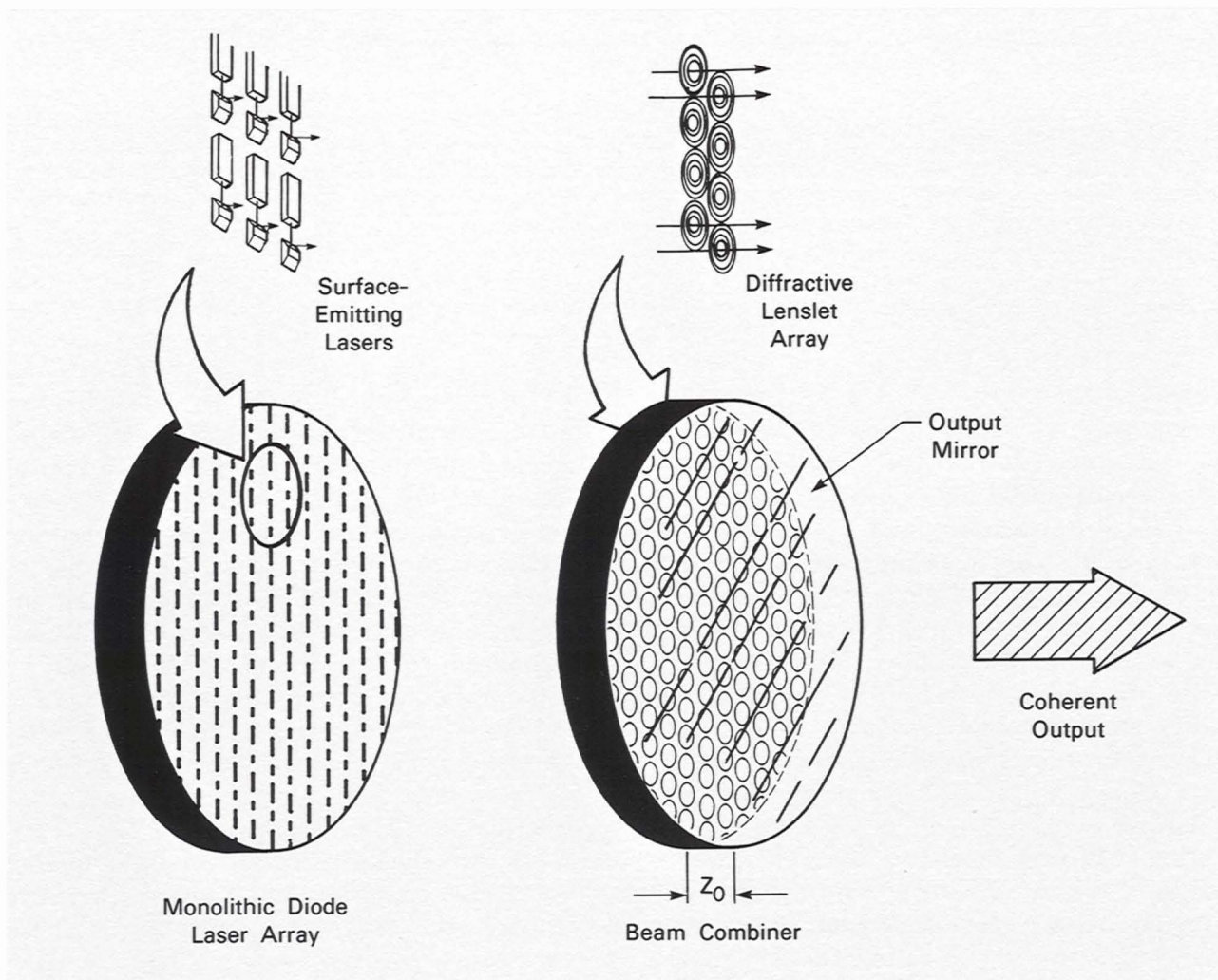
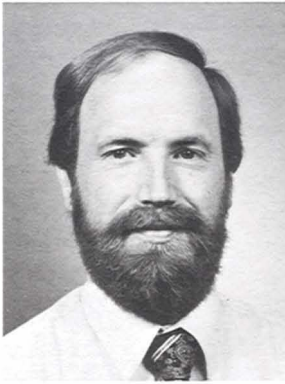


Fig. 12 — The CMC approach can be implemented on a single substrate by etching a microlens array into the front surface and depositing a partially reflecting output mirror on the back surface. The thickness of the substrate z_0 is chosen to satisfy the Talbot self-imaging condition. A thin spacer separates the beam combiner from the laser array.

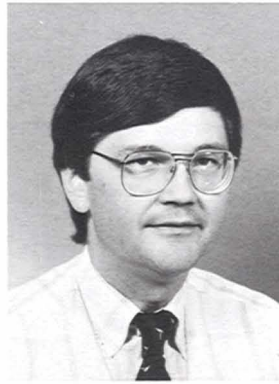
References

1. G.T. Forrest, "Diode-Pumped Solid-State Lasers Have Become a Mainstream Technology," *Laser Focus*, pg 62 (Nov. 1987).
2. D. Botez and D.E. Ackley, "Phase-Locked Arrays of Semiconductor Diode Lasers," *IEEE Circuits Devices Mag.* **2**, 8 (1986).
3. J.N. Walpole and Z.L. Liau, "Monolithic Two-Dimensional Arrays of High-Power GaInAsP/InP Surface-Emitting Diode Lasers," *Appl. Phys. Lett.* **48**, 1636 (1986).
4. J.P. Donnelly, W.D. Goodhue, T.H. Windhorn, R.J. Bailey, and S.A. Lambert, "Monolithic Two-Dimensional Surface-Emitting Arrays of GaAs/AlGaAs Diode Lasers," *Appl. Phys. Lett.* **51**, 1135 (1987).
5. J.J. Yang, M. Sergant, M. Jansen, S.S. Ou, L. Eaton, and W.W. Simmons, "Surface-Emitting GaAlAs/GaAs Linear Arrays with Etched Mirrors," *Appl. Phys. Lett.* **49**, 1138 (1986).
6. N.W. Carlson, G.A. Evans, J.M. Hammer, M. Lurie, S.L. Palfrey, and A. Dholakia, "Phase-Locked Operation of a Grating-Surface-Emitting Diode Laser Array," *Appl. Phys. Lett.* **50**, 1301 (1987).
7. J.R. Leger, G.J. Swanson, and W.B. Veldkamp, "Coherent Laser Addition Using Binary Phase Gratings," *Appl. Opt.* **26**, 4391 (1987).
8. H. Dammann and K. Goertler, "High-Efficiency In-Line Multiple Imaging by Means of Multiple Phase Holograms," *Opt. Commun.* **3**, 312 (1971).
9. J.R. Leger, G.J. Swanson, and W.B. Veldkamp, "Coherent Beam Addition of GaAlAs Lasers by Binary Phase Gratings," *Appl. Phys. Lett.* **48**, 888 (1986).
10. J. Harrison, G.A. Rines, P.F. Moulton, and J.R. Leger, "Coherent Summation of Injection-Locked Diode-Pumped Nd:YAG Ring Lasers," *Opt. Lett.* **13**, 111 (1988).
11. M. Holz, J.R. Leger, and G.J. Swanson, "Lossless Sidelobe Suppression for a Phase-Locked CO₂ Waveguide Array," *Conf. on Lasers and Electro-optics: Digest of Technical Papers* (Optical Society of America, New York, 1987), pg 356.
12. L.A. Newman and R.A. Hart, "Recent R&D Advances in Sealed-Off CO₂ Lasers," *Laser Focus*, pg 80 (June 1987).
13. L.A. Newman, R.A. Hart, J.T. Kennedy, A.J. Cantor, A.J. DeMaria, and W.B. Bridges, "High Power Coupled CO₂ Waveguide Laser Array," *Appl. Phys. Lett.* **48**, 1701 (1986).
14. J.R. Leger, G.J. Swanson, and M. Holz, "Efficient Side Lobe Suppression of Laser Diode Arrays," *Appl. Phys. Lett.* **50**, 1044 (1987).
15. D.F. Welsh, P. Cross, D. Scifres, W. Streifer, and R.D. Burnham, "In-Phase Emission from Index-Guided Laser Array up to 400 mW," *Electron. Lett.* **22**, 293 (1986).
16. J.R. Leger, M.L. Scott, P. Bundman, and M.P. Griswold, "Astigmatic Wavefront Correction of a Gain-Guided Laser Diode Array Using Anamorphic Diffractive Microlenses," *SPIE* **884**, 82 (1988).
17. W.H.F. Talbot, "Facts Relating to Optical Science. No. IV," *Philos. Mag.* **9**, 401 (1836).
18. Lord Rayleigh, "On Copying Diffraction-Gratings, and on Some Phenomena Connected Therewith," *Philos. Mag.* **11**, 196 (1881).
19. A.W. Lohmann and D.E. Silva, "An Interferometer Based on the Talbot Effect," *Opt. Commun.* **2**, 413 (1971).
20. J.R. Leger and M.A. Snyder, "Real-Time Depth Measurement and Display Using Fresnel Diffraction and White-Light Processing," *Appl. Opt.* **23**, 1655 (1984).
21. J.R. Leger, M.L. Scott, and W.B. Veldkamp, "Coherent Addition of AlGaAs Lasers Using Microlenses and Diffractive Coupling," *Appl. Phys. Lett.* **52**, 1771 (1988).



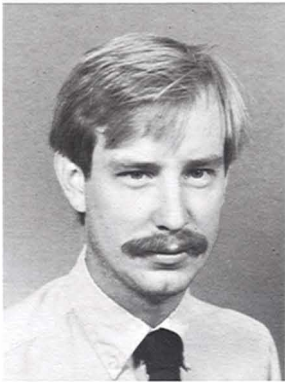
JAMES R. LEGER is a staff member in the Laser Radar Measurements Group. His research is focused on laser applications of diffractive optics. Before joining Lincoln Laboratory five years ago, Jim worked for 3M developing optical

techniques for robotics and automatic inspection. He received a BS in applied physics from CalTech and a PhD in applied physics from the University of California at San Diego.



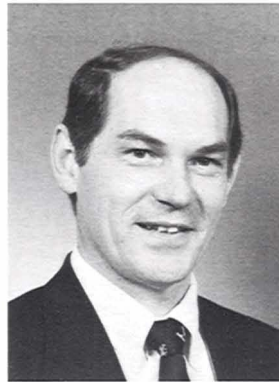
MICHAEL HOLZ is a staff member in the Laser Radar Measurements Group. His work spans the areas of binary optics, laser beam addition, laser physics, and neural networks. Before joining Lincoln Laboratory, Michael worked on a ring

laser gyroscope at Raytheon Research. He received a Physics Diploma from the Technical University of Munich and a PhD in physics from MIT. Michael encourages children to develop an appreciation of science; he performs science demonstrations at schools.



GARY J. SWANSON is a staff member in the Laser Radar Measurements Group, concentrating on binary optics. He has worked for

Lincoln Laboratory for six years. Gary received a BS in mathematics and a PhD in physics from the University of Michigan.



WILFRID B. VELDKAMP is Assistant Leader of the Laser Radar Measurements Group. He is involved in studies of sensor systems

technology, binary optics, and neural networks. Wilfrid received a BSc in electrical engineering from the University of Amsterdam and an EE/DSc in materials science and electrical engineering from MIT.